Indonesian Journal of Computing, Engineering, and Design

Journal homepage: http://ojs.sampoernauniversity.ac.id/index.php/IJOCED

Comparison of Heat Transfer Performance of Lattice-Structured Heat Sinks

Jerome Christo[1]*

[1]Department of Mechanical Engineering, Government College of Technology, Coimbatore, India

Correspondence: E-mail: jero.71772112146@gct.ac.in

ABSTRACT

This paper presents a comparative study of the heat transfer performance of lattice-structured heat sinks. Twenty different unit cells are chosen, and heat sinks are modeled in nTop with constant unit cell size. Al 6061 alloy is chosen as the material for analysis due to its good thermal conductivity, low weight, low cost, and high strength. Steady-state thermal analysis is performed using ANSYS with constant input parameters for all samples. Heat flux and temperature distribution within the heat sinks are analyzed. From the simulation, it was found that TPMS and plate-based heat sinks outperform other types with better heat transfer.

ARTICLE INFO

Article History:
Received 25 Jun 2024
Revised 29 Jul 2024
Accepted 26 Sep 2024
Available online 01 Oct 2024

Keywords:
Finite element analysis,
Heat sink,
Heat transfer,
Lattice structures,
Steady state thermal.

1. INTRODUCTION

Efficient heat transfer is crucial in various engineering applications, ranging from electronics cooling to HVAC systems, where enhancing heat dissipation capabilities can significantly improve system performance and reliability. Numerous studies have investigated the influence of fin geometry, such as shape (Arefin, 2016; Kushwaha et al., 2013), size, arrangement (Shah, 2016), and spacing (Yardi et al., 2017; Dewan et al., 2010), on heat transfer performance. Advancements in manufacturing techniques have enabled the fabrication of intricate fin designs to enhance heat transfer efficiency further (Catchpole-Smith et al., 2019). Lattice structures, drawing inspiration from the intricate patterns found in nature's cellular formations (Nazir et al., 2019), have been designed to overcome inherent fin shape and structure limitations. Lattice structures, characterized by their periodic arrangement of unit cells, possess distinct advantages such as high surface area-to-volume ratio, high strength-to-weight ratio (Perween et al., 2021), and low relative density. These attributes make lattice heat sinks promising candidates for efficient heat dissipation applications. However, comprehensive analyzes evaluating the thermal performance analyzes evaluating the thermal performance of lattice heat sink designs remain limited. This paper presents a systematic investigation into the heat transfer characteristics of heat sinks with lattice structures using numerical analysis.

2. LATTICE STRUCTURES

Lattice structures, also known as architected cellular materials, are a type of cellular structure with repeating unit cells (Dong et al., 2017). Certain physical properties of lattice structures can be tailored by controlling their geometrical parameters (Schaedler & Carter, 2016). Some lattice structures, e.g., lattice metamaterials, exhibit unique characteristics (Talebi et al., 2021) such as negative Poisson ratio (Bhate & Hayduke, 2023), negative compressibility, negative thermal expansion, phononic band gap, etc., which make them useful for a wide range of applications, including light-weighting, energy absorption, bio-scaffolds, noise/vibration wave insulation, and thermal management (Jia et al., 2020). Lattice structures have been found to break the parasitic performance trade-offs (Jia et al., 2019) seen in bulk materials such as strength vs. toughness (Ritchie, 2011; Bouville et al., 2014), stiffness vs. energy dissipation, flexibility vs. fast response, etc. The lattice structures' high surface area to volume ratio makes them an ideal choice for high-performance heat exchanger applications. Powered by the rapid development of additive manufacturing techniques, compact lattice heat sinks may soon replace traditional heat sink types.

Based on the type and arrangement of unit cells, lattice structures are grouped into many classes (Benedetti et al., 2021; Pei et al., 2022; Abou-Ali et al., 2022; Guo et al., 2019; Tancogne-Dejean et al., 2018; Andrew et al., 2021; Pronk et al., 2017; McGregor et al., 2021; Tyagi et al., 2023; Andrei et al., 2021) as shown in **Figure 1** (unit cell-based) and **Figure 2** (periodicity-based).

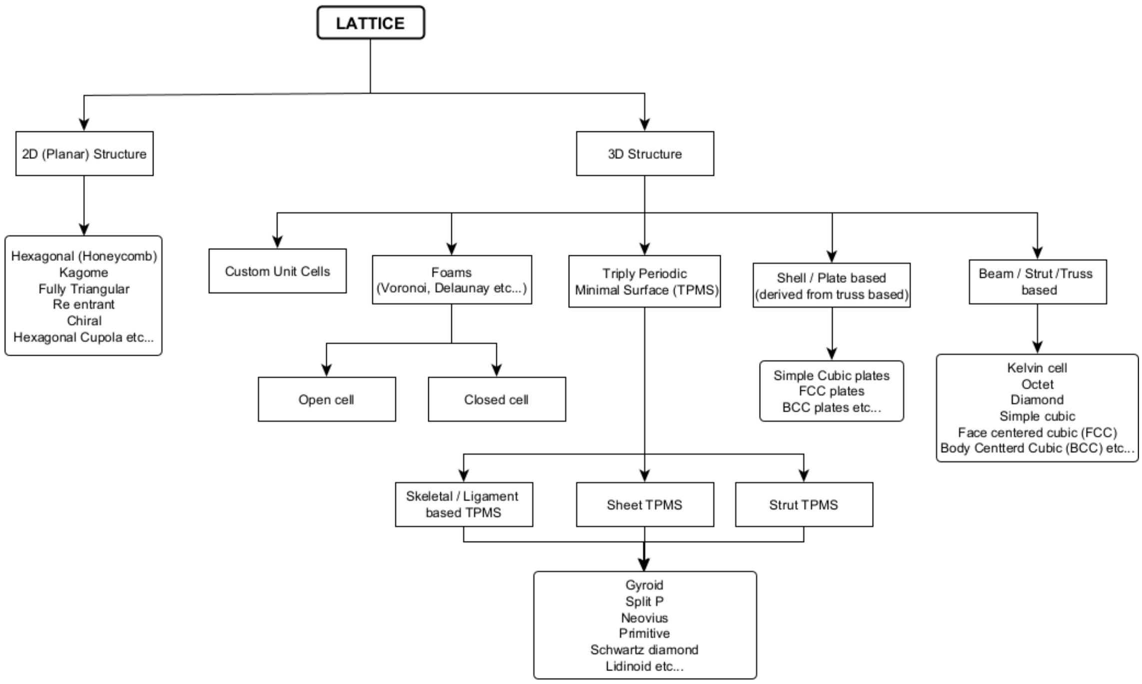

Figure 1. Classification of lattice structures based on unit cell

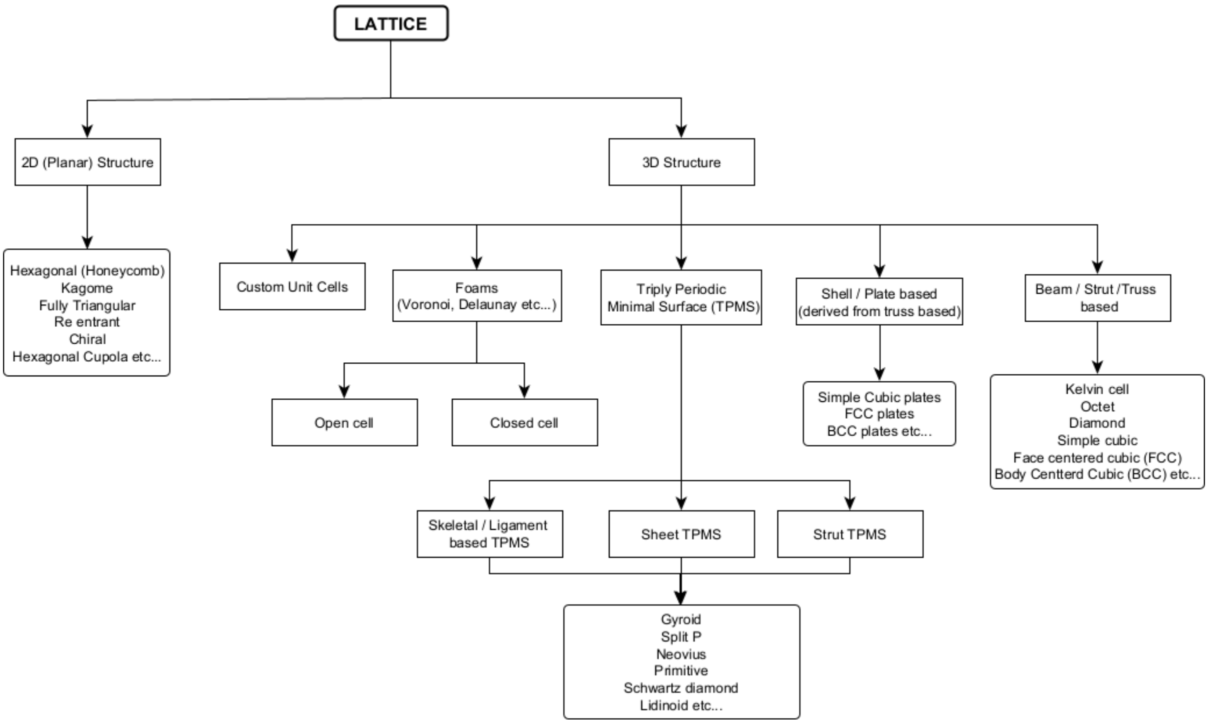

Figure 2. Classification of lattice structures based on periodicity

3. METHODOLOGY

3.1. Geometric Modelling

The fins are modeled using nTop, an implicit modeling software. Unlike explicit modeling techniques, which represent a body as a set of polygons or parametric patches (Opalach & Maddock, 1995), implicit modeling technique distinguishes between points inside and outside a body by representing them as a function or scalar field (Fayolle et al., 2017). This allows for creating complex shapes and features that are otherwise impossible to model with explicit modeling software. Implicit modeling is also ideal for designing additively manufactured parts. However, implicit models require significantly high computational resources and are not the ideal method to represent 3d models for subtractive manufacturing, as calculating the boundary of the slice is a complicated process (Li et al., 2018). All fins taken for analysis possess similar basic dimensions, shown in **Figure 3**. The unit cells selected for analysis are depicted in **Figure 4**, **Figure 5**, and **Figure 6**. Constant unit cell sizes are used throughout the analysis. The unit cells chosen for analysis are shown in **Figure 4** for beam/truss-based unit cells, **Figure 5** for 2D and plate-based unit cells, and **Figure 6** for triply periodic minimal surface (TPMS) unit cells. All unit cells are of the following dimensions: 15mm x 20mm x 20mm.

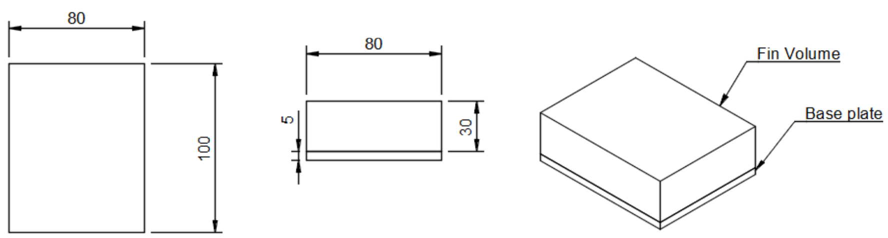

Figure 3. Basic heat sink dimensions

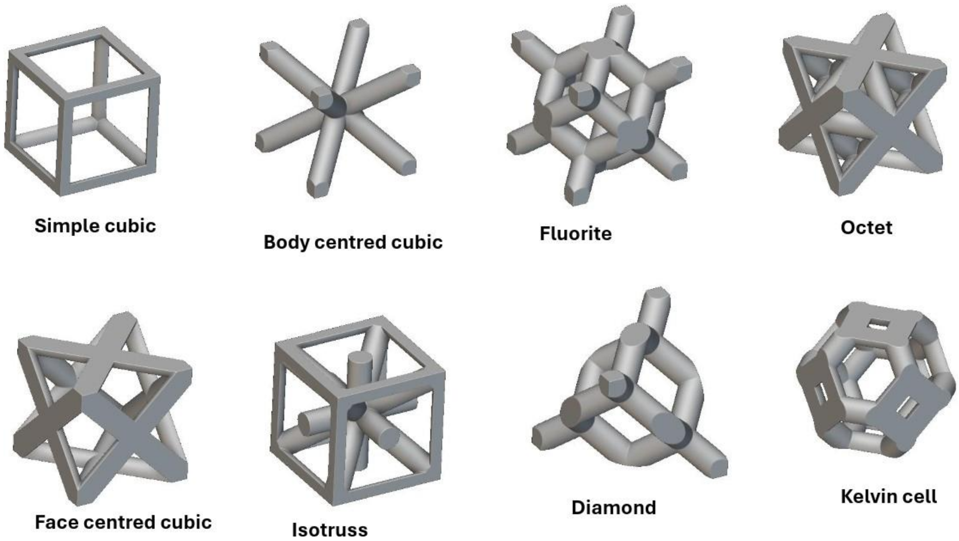

Figure 4. Beam/Truss-based unit cells.

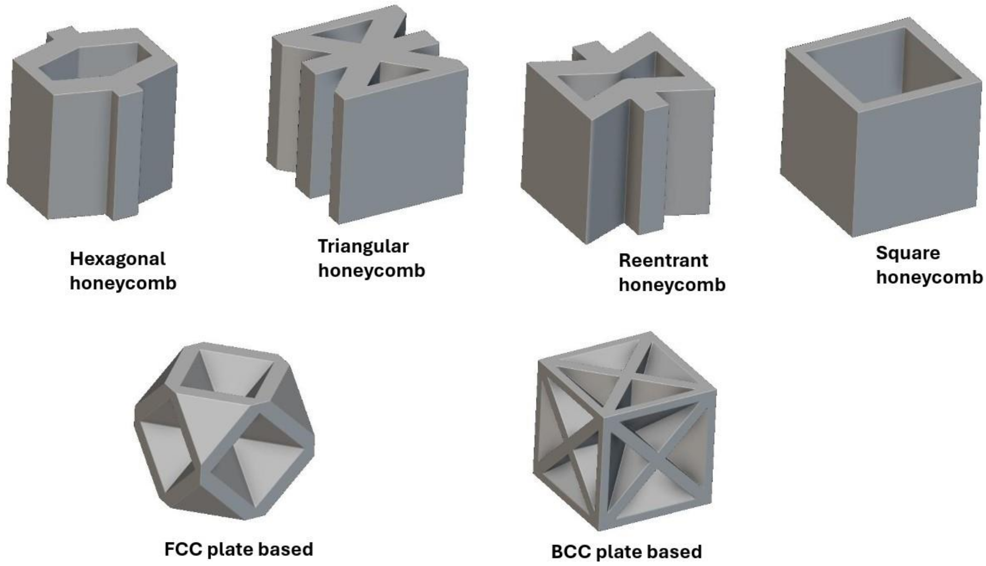

Figure 5. 2D and plate-based unit cells.

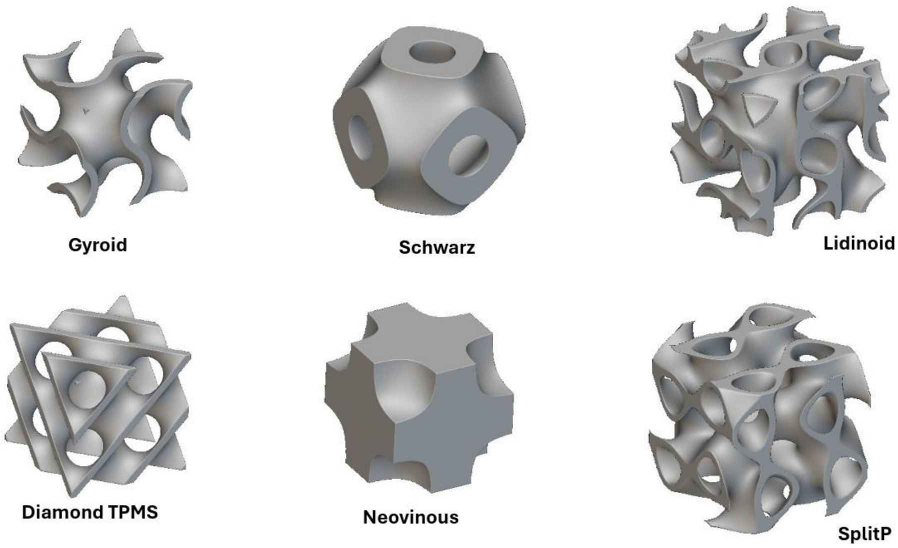

Figure 6. TPMS unit cells

3.2. Finite Element Analysis

The steady-state thermal analysis is carried out using ANSYS. In steady-state analysis, the object under study is assumed to be in equilibrium, and ambient conditions are also assumed to be constant. The same material properties and boundary conditions are defined for all heat sink types. The material is assumed to be isotropic and homogeneous with constant thermal conductivity.

3.2.1. Material Properties

Aluminium alloys are typically preferred for heat sinks due to their excellent thermal conductivity, low weight, low cost, and high strength. Al 6000 series alloys are widely used as they can be extruded easily. Al 6061 alloy is taken for analysis. Some essential properties of Al 6061 alloy are given below:

- Material: Al 6061 T6
- Density: 2713 kg/m^3
- Poisson's Ratio: 0.33
- Young's modulus: 6.904E+10 Pa
- Bulk modulus: 6.7686E+10 Pa
- Isotropic Thermal Conductivity: 155.3 W/m.K
- Ultimate Tensile strength: 3.131E+8 Pa
- Specific Heat (constant Pressure): 915.7 J/kg.K
- Isotropic Secant Coefficient of Thermal Expansion: 2.278E-5 /K
- Composition of Al 6061 alloy is shown in **Table 1**.

Table 1. Material composition (Al 6061).

Element	Wt. %
Al	95.898.6
Cr	0.040.35
Cu	0.150.4
Fe	Max 0.7
Mg	0.81.2
Mn	Max 0.15
Si	0.40.8
Ti	Max 0.15
Zn	Max 0.25

3.2.2. Boundary Conditions

In this study, a constant film coefficient is assumed for simplicity. In actual practice, the film coefficient of a heat sink depends on various factors, such as surface roughness, geometrical parameters, fluid properties (viscosity, density), flow rate, heat flux, temperature gradient, etc. (Moreira et al., 2019). Additionally, obtaining an accurate value of the heat transfer coefficient is difficult as it changes locally and temporally (Grądziel et al., 2019; Bury & Hanuszkiewicz-Drapala, 2018; Erdoğdu, 2008; D. V. Abramkina et al., 2018; Korprasertsak & Leephakpreeda, 2017). Heat transfer due to radiation is neglected. A constant heat input of 100W is given in the bottom face of the base plate (**Figure 7(a)**) and convection boundary conditions is applied in the sample (**Figure 7(b)**).

The following boundary conditions are defined, as follows: Film coefficient is 25 W/m^2 K, heat flow(base) is 100 W, and ambient temperature is 30^0 C. The heat sink data is shown in **Table 2** and mass vs surface area plot is shown in **Figure 8**.

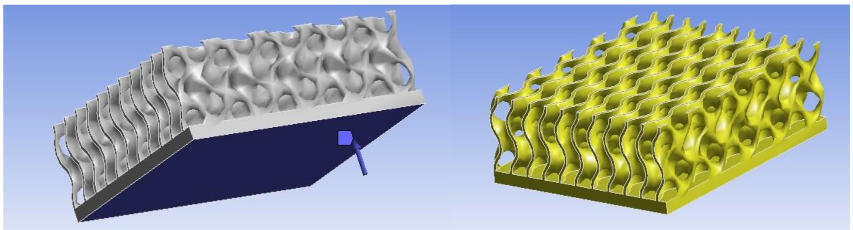

(a) (b)

Figure 7(a). Heat flow (input) boundary (b). Convection boundary

Table 2. Heat Sink Data

Unit cell type	Thickness (mm)	Nodes	Ele-ments	Mass(g)	Surface area (mm²)	Wt. %
Simple cubic	4	223143	138108	173.74	44571.33	22.87136012
Body centered cubic	3	279253	162839	191.86	55570.87	25.25670054
Face centered cubic	3	321148	187137	208.27	66091.82	27.41693434
Diamond	3	304447	181469	191.64	55724.85	25.22773946
Octet	3	526883	316205	291.18	98070.46	38.33131483
Kelvin cell	3	303670	177447	206.2	62850.66	27.14443684
Fluorite	3	438067	258296	260.78	82638.74	34.3294192
Isotruss	3	219156	136626	253.29	81405.53	33.34342583
Triangular hon-eycomb	3	343357	224716	494.2	96459.57	65.05713233
Hexagonal hon-eycomb	3	29284	122089	355	74245.7	46.73266284
Reentrant hon-eycomb	3	219977	135062	417.63	87043.11	54.9773577
Square honey-comb	3	123582	74924	289.2	60256.69	38.07066505
FCC plate	1	428251	253213	326.36	155390.4	42.9624559
BCC plate	1	477545	296874	370.86	180576.59	48.82049392
Gyroid	2	197347	103200	247.82	102846.45	32.6233479
Schwarz	2	207814	121741	350.62	79234.29	46.15607393
Diamond TPMS	2	226259	116393	275.64	120721.57	36.28560897
Lidinoid	2	281184	166176	360.86	157632.11	47.50408088
SplitP	2	609100	325740	295.65	152601.96	38.91975146
Neovinous	1	866475	597273	422.76	74812.35	55.65267758

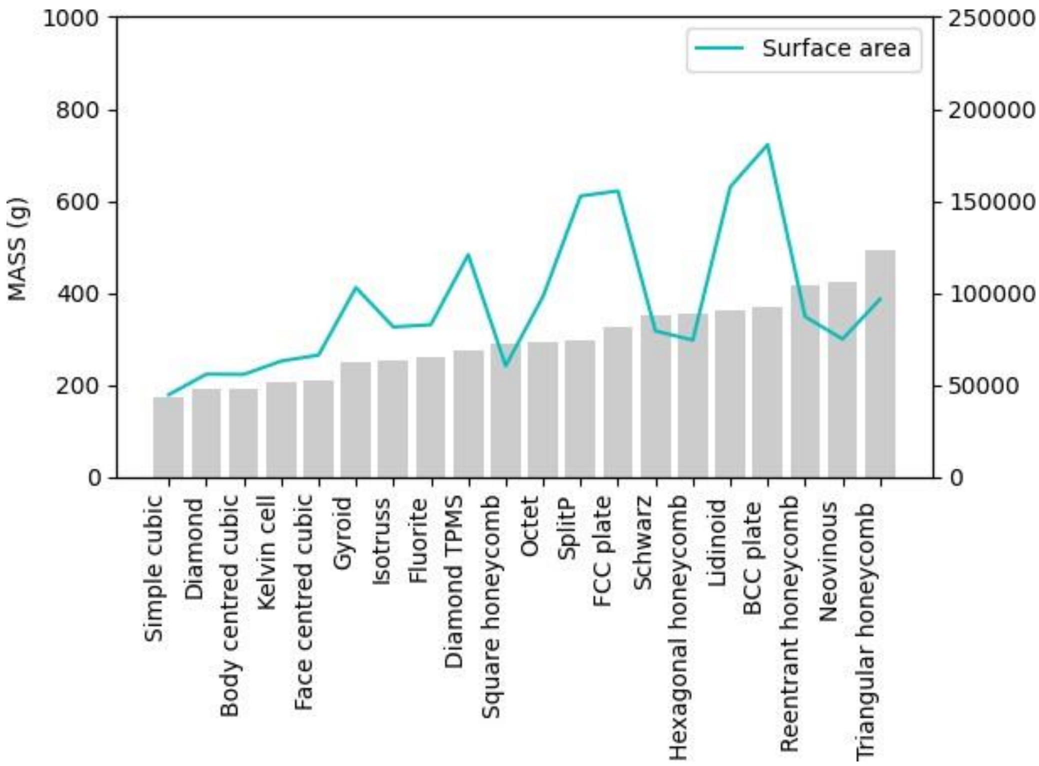

Figure 8. Mass vs Surface area plot

4. RESULTS AND DISCUSSION

Table 3 shows the values of temperature and heat flux from the simulation. The highest temperature difference within the simple cubic heat sink. However, the maximum temperature produced in the simple cubic heat sink is the highest among all types taken for analysis, which may limit its practical applications. The maximum temperature reached in plate-based heat sinks is lower than in other types. In most cases, the temperature difference increases with the decreasing mass of the heat sink with the same film coefficient (**Figure 9**).

Figure 10 show the temperature distribution in the various unit cell. Temperature distribution in the 2D lattice structured heat sinks is not uniform along the vertical axis and changes based on the unit cell orientation. **Figure 11** show the heat flux distribution of the various unit cell type. A more uniform heat flux distribution is seen in 2D, honeycomb, and TPMS lattices than in beam/truss-based structures.

Figure 12 shows the minimum and maximum temperature for the various unit cell. It can be seen that the simple cubic has the highest maximum temperature. In addition, the simple cubic has also the highest heat flux (**Figure 13**). Mass and temperature difference plot is shown in **Figure 14**. Temperature difference against surface area plot is shown in **Figure 15**. The results are highly subject to the design parameters of unit cells and the heat transfer coefficient. For a given value of film coefficient, beam/truss-based heat sinks outperform other types in terms of mass and temperature difference produced. Future works may analyze the heat transfer properties of heat sinks with film coefficient obtained using computational fluid dynamic (CFD) analysis results.

Table 3. Analysis results of various unit cell types

Unit cell type	Min. temp. (^{0}C)	Max. temp. (^{0}C)	Temperature difference (^{0}C)	Min heat flux (W/m^2)	Max. heat flux (W/m^2)
Simple cubic	104.16	176.89	72.73	365.95	5.61E+05
Body centered cubic	89.87	144.43	54.56	99.05	4.82E+05
Face centered cubic	75.89	128.43	52.54	171.42	2.43E+05
Diamond	86.84	144.33	57.49	41.645	4.31E+05
Octet	64.18	90.85	26.67	41.633	1.34E+05
Kelvin cell	83.23	129.14	45.91	175.63	4.17E+05
Fluorite	71.93	101.24	29.31	56.76	3.00E+05
Isotruss	69.61	104.44	34.83	135.36	2.29E+05
Triangular honeycomb	72.54	80.04	7.5	572.32	50991
Hexagonal honeycomb	85.58	95.22	9.64	246.49	1.29E+05
Reentrant honeycomb	76.86	86.59	9.73	195.95	99972
Square honeycomb	104.63	109.75	5.12	654.98	69641
FCC plate	52.44	66.94	14.5	143.12	99131
BCC plate	49.34	61.32	11.98	53.9	1.00E+05
Gyroid	64.4	84.07	19.67	149.76	1.23E+05
Schwarz	80.96	93.69	12.73	219.91	1.44E+05
Diamond TPMS	58.67	74.94	16.27	107.53	1.57E+05
Lidinoid	66.23	76.42	10.19	135.47	64755
SplitP	51.46	66.83	15.37	67.57	1.82E+05
Neovinous	86.51	95.77	9.26	129.53	72583

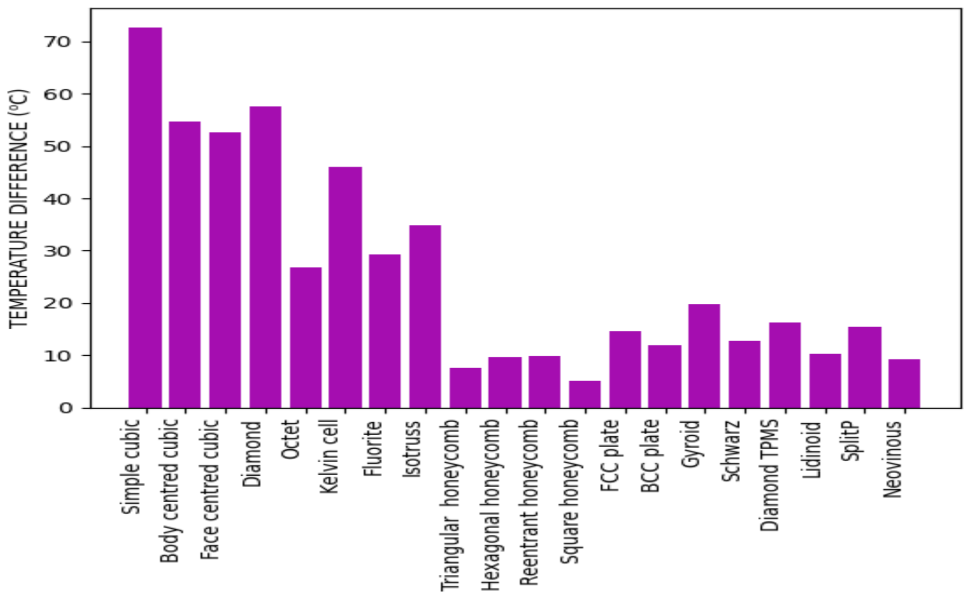

Figure 9. Temperature difference

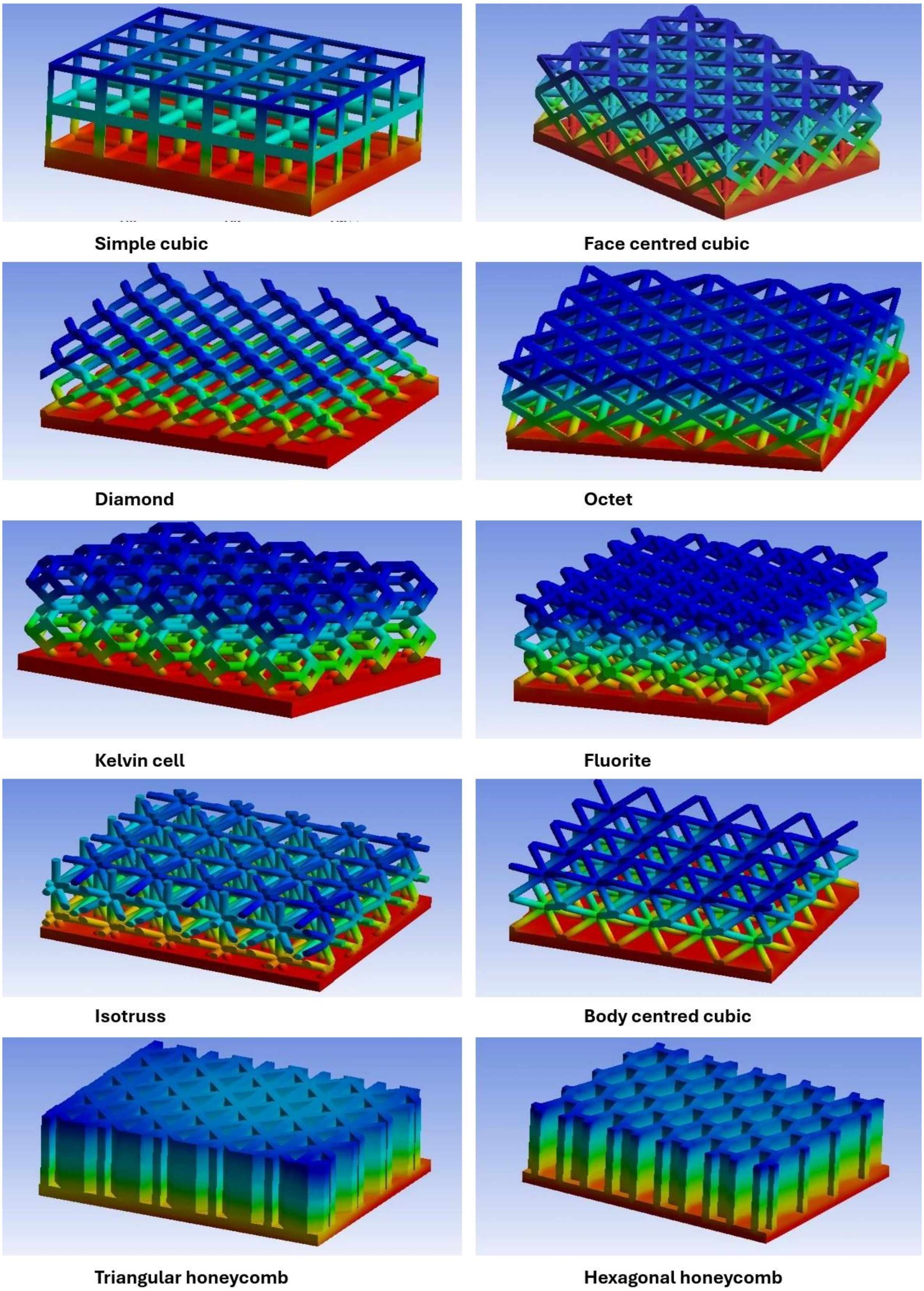

Figure 10. Temperature distribution results

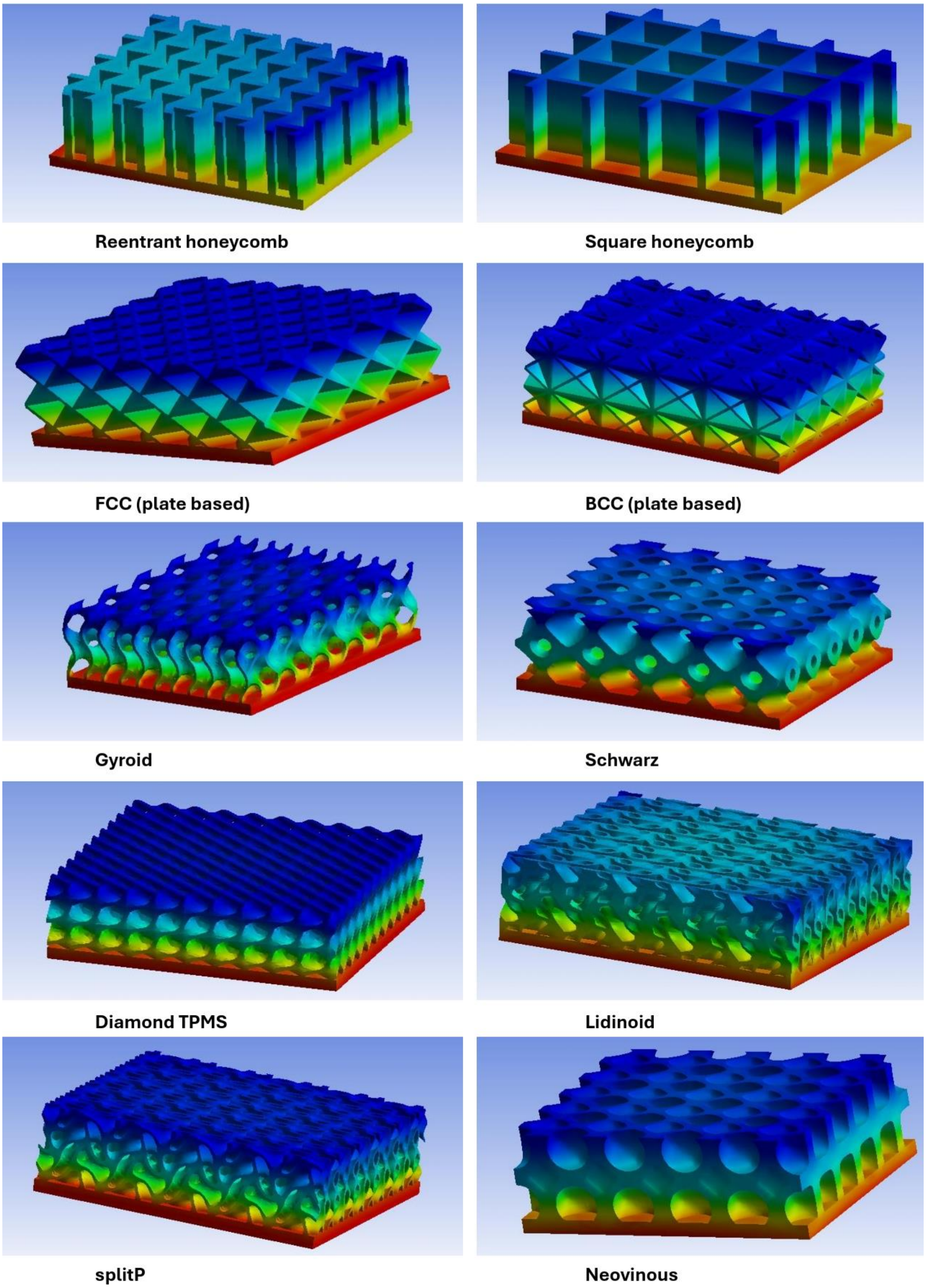

Figure 10. Temperature distribution results (continued)

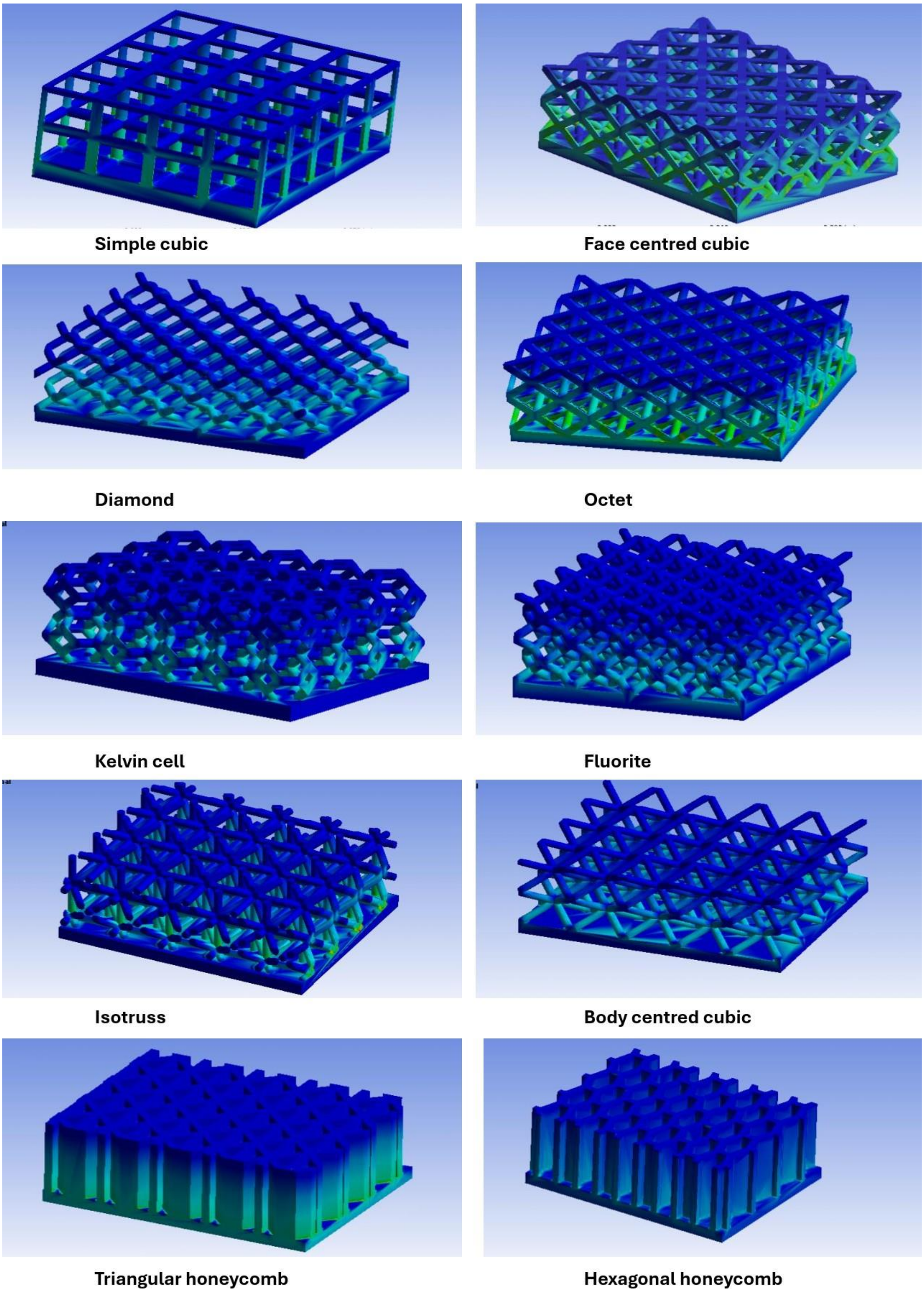

Figure 11. Heat flux distribution

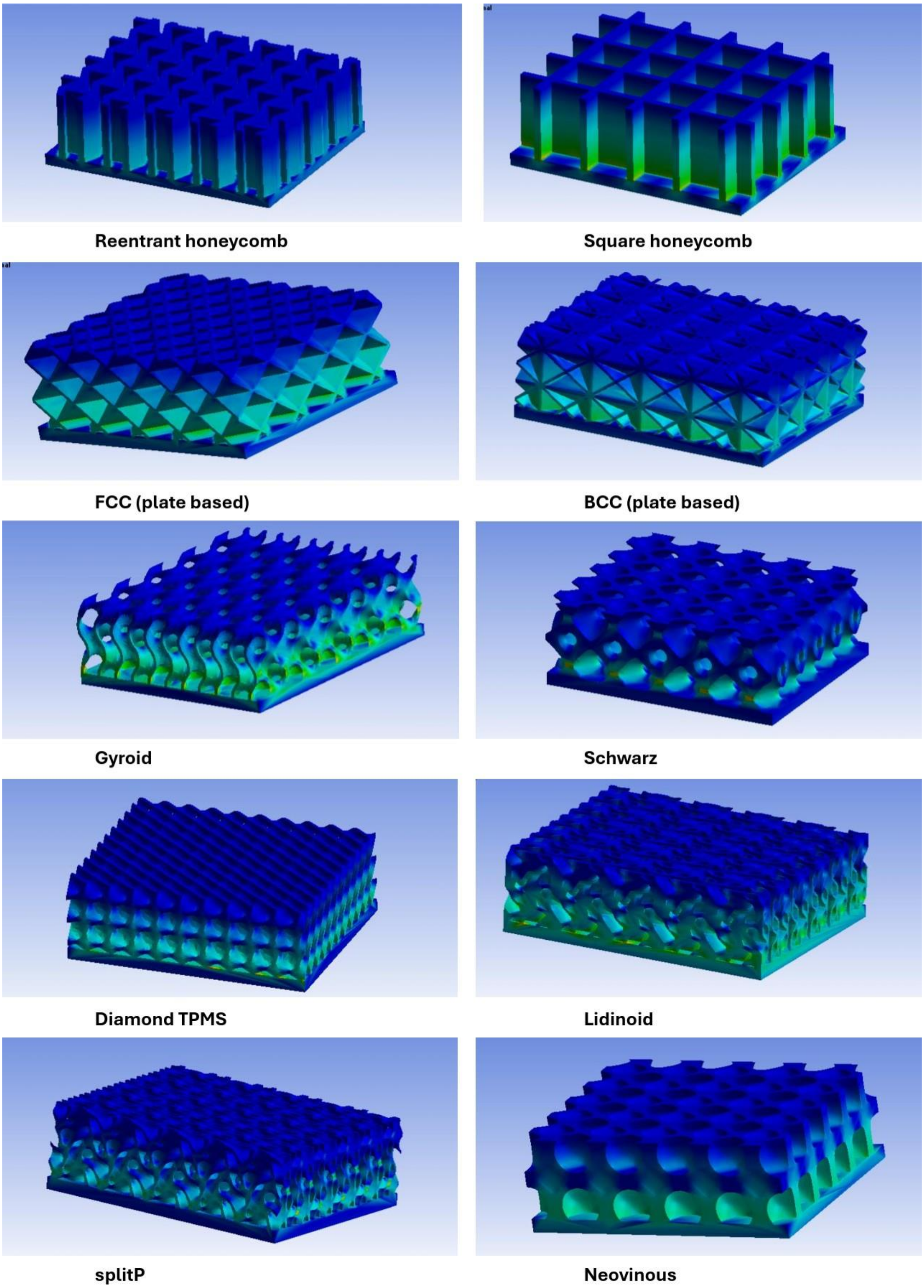

Figure 11. Heat flux distribution (continued)

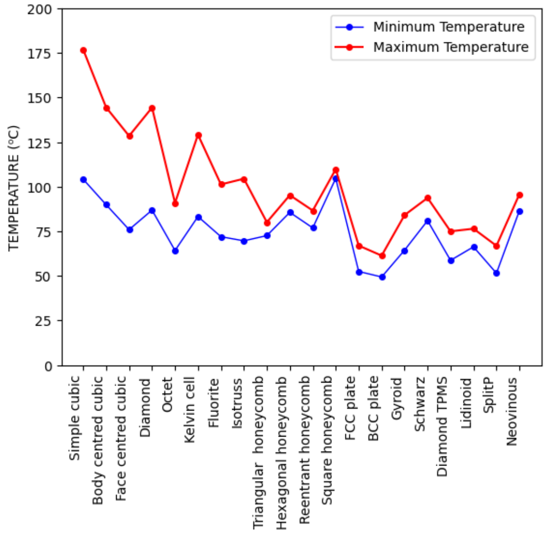

Figure 12. Minimum and maximum temperatures plot

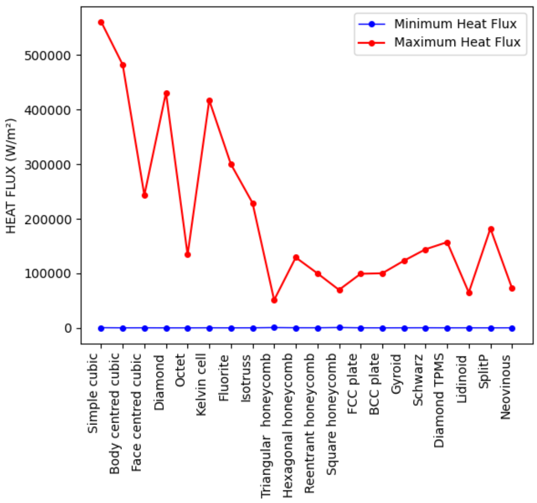

Figure 13. Minimum and maximum heat flux plot

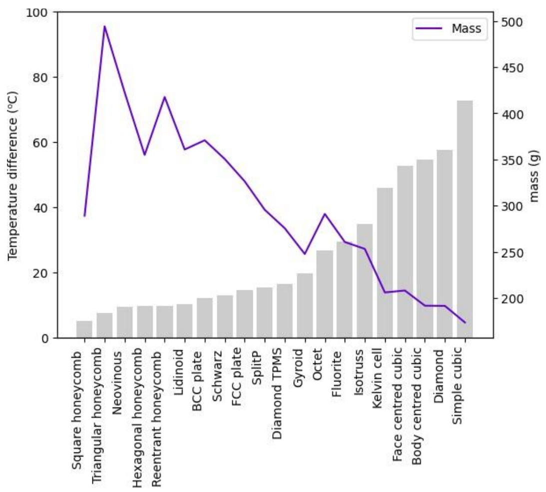

Figure 14. Mass vs Temperature difference plot

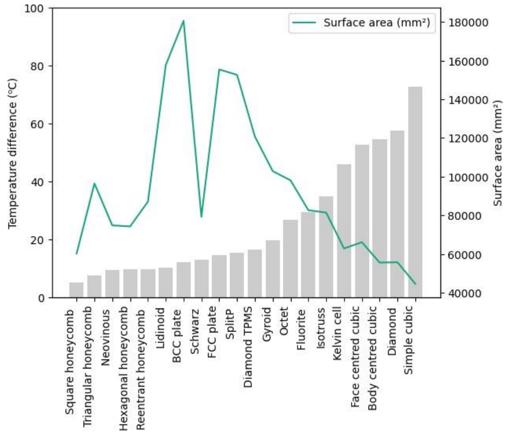

Figure 15. Temperature difference vs surface area plot

5. CONCLUSION

Various unit cell has been tested in order to identify their performance in heat transfer process. The steady state thermal analysis using ANSYS simulation is conducted. The results interpret that TPMS, and plate-based heat sinks have better overall performance due to their higher surface area and more significant temperature gradient. They also possess a low mass density.

ACKNOWLEDGEMENT

The author expresses his sincere gratitude to nTop (formerly nTopology) for providing free access to their state-of-the-art software, significantly facilitating his research endeavors. I would also like to thank Autodesk (Fusion) and ANSYS for their exceptional products.

REFERENCES

Abou-Ali, A., Lee, D.-W., & Abu Al-Rub, R. (2022). On the Effect of Lattice Topology on Mechanical Properties of SLS Additively Manufactured Sheet-, Ligament-, and Strut-Based Polymeric Metamaterials. *Polymers*, *14*, 4583. https://doi.org/10.3390/polym14214583

Andrew, J., Alhashmi, H., Schiffer, A., Kumar, S., & Deshpande, V. (2021). Energy absorption and self-sensing performance of 3D printed CF/PEEK cellular composites. *Materials & Design*, *208*, 109863. https://doi.org/10.1016/j.matdes.2021.109863

Arefin, A. M. E. (2016). Thermal analysis of modified pin fin heat sink for natural convection. *2016 5th International Conference on Informatics, Electronics and Vision (ICIEV)*, 1–5. https://doi.org/10.1109/ICIEV.2016.7759986

Benedetti, M., du Plessis, A., Ritchie, R. O., Dallago, M., Razavi, N., & Berto, F. (2021). Architected cellular materials: A review on their mechanical properties towards fatigue-tolerant design and fabrication. *Materials Science and Engineering: R: Reports*, *144*, 100606. https://doi.org/https://doi.org/10.1016/j.mser.2021.100606

Bhate, D., & Hayduke, D. (2023). Architected Cellular Materials. In M. Seifi, D. L. Bourell, W. Frazier, & H. Kuhn (Eds.), *Additive Manufacturing Design and Applications* (Vol. 24A, p. 0). ASM International. https://doi.org/10.31399/asm.hb.v24A.a0006951

Bouville, F., Maire, E., Meille, S., Van de Moortèle, B., Stevenson, A. J., & Deville, S. (2014). Strong, tough and stiff bioinspired ceramics from brittle constituents. *Nature Materials*, *13*(5), 508–514. https://doi.org/10.1038/nmat3915

Bury, T., & Hanuszkiewicz-Drapala, M. (2018). Evaluation of selected methods of the heat transfer coefficient determination in fin-and-tube cross-flow heat exchangers. *MATEC Web of Conferences*, *240*, 2004. https://doi.org/10.1051/matecconf/201824002004

Catchpole-Smith, S., Sélo, R., Davis, A. W., Ashcroft, I., Tuck, C., & Clare, A. (2019). Thermal Conductivity of TPMS Lattice Structures Manufactured via Laser Powder Bed Fusion. *Additive Manufacturing*, *30*, 100846. https://doi.org/10.1016/j.addma.2019.100846

D. V. Abramkina, Abramyan, A. A., & Shevchenko-Enns, E. R. (2018). Experimental determination of convective heat transfer coefficients in thermal buoyacy ventilation system. *Herald of Dagestan State Technical University.*, *45*(4), 133–144.

Dewan, A., Patro, P., Khan, I., & Mahanta, P. (2010). The effect of fin spacing and material on the performance of a heat sink with circular pin fins. *Proceedings of The Institution of Mechanical Engineers Part A-Journal of Power and Energy - PROC INST MECH ENG A-J POWER*, *224*, 35–46. https://doi.org/10.1243/09576509JPE750

Dong, G., Tang, Y., & Zhao, Y. F. (2017). A Survey of Modeling of Lattice Structures Fabricated by Additive Manufacturing. *Journal of Mechanical Design*, *139*(10). https://doi.org/10.1115/1.4037305

Erdoğdu, F. (2008). A review on simultaneous determination of thermal diffusivity and heat transfer coefficient. *Journal of Food Engineering*, *86*(3), 453–459. https://doi.org/https://doi.org/10.1016/j.jfoodeng.2007.10.019

Fayolle, P. A., Fryazinov, O., & Pasko, A. (2017). Rounding, filleting and smoothing of implicit surfaces. *Computer-Aided Design and Applications*, *15*, 1–10.

https://doi.org/10.1080/16864360.2017.1397890

Grądziel, S., Majewski, K., & Majdak, M. (2019). Experimental determination of the heat transfer coefficient in internally rifled tubes. *Thermal Science*, *23*, 1163–1174. https://doi.org/10.2298/TSCI19S4163G

Guo, X., Zheng, X., Yang, Y., Yang, X., & Yi, Y. (2019). Mechanical behavior of TPMS-based scaffolds: a comparison between minimal surfaces and their lattice structures. *SN Applied Sciences*, *1*(10), 1145. https://doi.org/10.1007/s42452-019-1167-z

Jia, Z., Liu, F., Jiang, X., & Wang, L. (2020). Engineering lattice metamaterials for extreme property, programmability, and multifunctionality. *Journal of Applied Physics*, *127*, 150901. https://doi.org/10.1063/5.0004724

Jia, Z., Yu, Y., & Wang, L. (2019). Learning from nature: Use material architecture to break the performance tradeoffs. *Materials and Design*, *168*, 107650. https://doi.org/10.1016/j.matdes.2019.107650

Korprasertsak, N., & Leephakpreeda, T. (2017). Real-Time Determination of Convective Heat Transfer Coefficient Via Thermoelectric Modules. *Journal of Heat Transfer*, *139*. https://doi.org/10.1115/1.4036734

Kushwaha, A. S. & Kirar, R. (2013). Comparative Study of Rectangular, Trapezoidal and Parabolic Shaped Finned Heat sink. *IOSR Journal of Mechanical and Civil Engineering*, *5*, 1–7. https://doi.org/10.9790/1684-0560107

Li, Q., Hong, Q., Qi, Q., ma, X., Han, X., & Tian, J. (2018). Towards additive manufacturing oriented geometric modeling using implicit functions. *Visual Computing for Industry, Biomedicine, and Art*, *1*. https://doi.org/10.1186/s42492-018-0009-y

McGregor, Martine, Sagar Patel, Stewart McLachlin, and Mihaela Vlasea. "Architectural bone parameters and the relationship to titanium lattice design for powder bed fusion additive manufacturing." Additive Manufacturing 47 (2021): 102273. http://dx.doi.org/10.1016/j.addma.2021.102273

Moreira, T., Colmanetti, A. R., & Tibiriçá, C. (2019). Heat transfer coefficient: a review of measurement techniques. *Journal of the Brazilian Society of Mechanical Sciences and Engineering*, *41*, 264. https://doi.org/10.1007/s40430-019-1763-2

Nazir, A., Mekonen, K., Kumar, A., & Jeng, J.-Y. (2019). A state-of-the-art review on types, design, optimization, and additive manufacturing of cellular structures. *The International Journal of Advanced Manufacturing Technology*, *104*. https://doi.org/10.1007/s00170-019-04085-3

Opalach, A., & Maddock, S. (1995). *An Overview of Implicit Surfaces*.

Pei, E., Kabir, I., Breški, T., Godec, D., & Nordin, A. (2022). A review of geometric dimensioning and tolerancing (GD&T) of additive manufacturing and powder bed fusion lattices. *Progress in Additive Manufacturing*, *7*. https://doi.org/10.1007/s40964-022-00304-8

Perween, S., Fahad, M., & Khan, M. (2021). Systematic Experimental Evaluation of Function Based Cellular Lattice Structure Manufactured by 3D Printing. *Applied Sciences*, *11*, 10489. https://doi.org/10.3390/app112110489

Pronk, T. N., Ayas, C., & Tekoğlu, C. (2017). A Quest for 2D Lattice Materials for Actuation. *Journal of the Mechanics and Physics of Solids*, *105*. https://doi.org/10.1016/j.jmps.2017.05.007

Ritchie, R. O. (2011). The conflicts between strength and toughness. *Nature Materials*, *10*(11), 817–822. https://doi.org/10.1038/nmat3115

Schaedler, T. A., & Carter, W. B. (2016). Architected Cellular Materials. *Annual Review of Materials Research*, *46*(Volume 46, 2016), 187–210. https://doi.org/https://doi.org/10.1146/annurev-matsci-070115-031624

Shah, S. I. (2016). Effect of geometry and arrangement of pin fin in heat exchanger: A review. *International Journal of Emerging Technologies and Innovative Research*, *3*(2), 39–43.

Talebi, S., R. Hedayati, and M. Sadighi. "Dynamic crushing behavior of closed-cell aluminum foams based on different space-filling unit cells." Archives of Civil and Mechanical Engineering 21, no. 3 (2021): 99. http://dx.doi.org/10.1007/s43452-021-00251-1

Tancogne-Dejean, T., Diamantopoulou, M., Gorji, M. B., Bonatti, C., & Mohr, D. (2018). 3D Plate-Lattices: An Emerging Class of Low-Density Metamaterial Exhibiting Optimal Isotropic Stiffness. *Advanced Materials*, *30*(45), 1803334. https://doi.org/https://doi.org/10.1002/adma.201803334

Tyagi, Shivank A., and M. Manjaiah. "Additive manufacturing of titanium-based lattice structures for medical applications–a review." Bioprinting 30 (2023): e00267. https://doi.org/10.1016/j.bprint.2023.e00267

VOICU, Andrei Daniel, Anton Hadăr, and Daniel Vlăsceanu. "Benefits of 3D printing technologies for aerospace lattice structures." *Scientific Bulletin'Mircea cel Batran'Naval Academy 24*, no. 1 (2021). http://dx.doi.org/10.21279/1454-864X-21-I1-001

Yardi, A., Karguppikar, A., Tanksale, G., & Sharma, K. (2017). Optimization of fin spacing by analyzing the heat transfer through rectangular fin array configurations (natural convection). *International Research Journal of Engineering and Technology*, *4*(9).